

## COMPUTATIONAL MODELING AND STATISTICAL ANALYSIS ON THE CORROSION INHIBITION OF ALUMINIUM IN NITRIC ACID SOLUTION BY ETHANOLIC EXTRACT OF *CITRUS SINESIS* SEED

Chimezie P. Ozoemena<sup>1\*</sup> and Milam Charles<sup>1</sup>

<sup>1</sup>Department of Chemistry, University of Uyo, Akwa Ibom State, Nigeria

<sup>1</sup>Department of Chemistry, Moddibo Adama University of Technology, Adamawa State, Nigeria

---

**ABSTRACT:** *The purpose of this paper is to study the inhibition potential of ethanol extract of Citrus Sinesis Seed (CSS) on the corrosion of mild steel in 1M HCl using phytochemical screening, conventional weight loss, scanning electron microscopy (SEM), fourier transform infrared spectroscopy (FTIR) and Quantum chemical analysis. The experimental results revealed that the Inhibition efficiency of the Citrus Sinesis seed extract increases with extracts concentration but decreases with time and temperature. The inhibition efficiency increases gradually reaching a maximum value of 96.72% within the first 2 hours at a concentration of 1.0g/l. the extract acts as an inhibitor because of its phytochemical composition and is adsorbed spontaneously on the surface of aluminium according to Langmuir adsorption isotherm. The mechanism of physical adsorption is proposed from the inhibition efficiency with temperature and the values of some kinetic and thermodynamic parameters were obtained. FTIR results showed that the inhibition mechanism was an absorption process through the functional groups present in the seed extract. Surface morphology also revealed that corrosion product confirmed the protection offered by the extract on the surface of the metal immersed in the acid media. Quantum chemical studies confirmed that inhibition was due to adsorption of active molecules leading to formation of a protective layer on surface of mild steel.*

**KEY WORDS:** corrosion, corrosion inhibitors, mild steel, weight loss, scanning electron microscopy quantum analysis

---

### INTRODUCTION

Industrial development is paramount in the history of any developed nation. Aluminium and its alloy are widely used in industries because of their light weight and good resistance to corrosion in cooling water systems, for shipboard condensers, power plant condensers, transportation, consumer goods, and electrical products. Aluminium and its alloy are very interesting because of its great industrial importance. Acid solutions especially nitric acid are used for industrial processes such as industrial cleaning agent and acid descaling, etching of metals, scrubbing, as well as oil well acid in oil recovery and pickling of metal structures. In most cases, contact between the metals and acidic media exposed industrial facilities to corrosion and therefore constitute a great problem with adverse economic implication costing billions of dollars each year. In view of the

above, the use of inhibitors of organic origin has been found to be one of the best options available irrespective of other several options (painting, electroplating, and oiling) for the protection of metals against corrosion (Oguzie *et al.*, 2006, Awe *et al.*, 2015). For these organic compounds, their adsorption on the metal surface is the initial step of inhibition and occur due to the presence of heteroatoms such as oxygen, nitrogen, sulfur, phosphorus and conjugated diene as well as triple bond or aromatic ring in their molecular structure (Peter *et al.*, 2016, Banu *et al.*, 2016, EL-Basiony *et al.*, 2019). Synthetic organic compounds have been used as efficient corrosion inhibitors but are highly toxic, expensive couple with environmental pollution. In light of these, several plant have plant extracts have been investigated and corrosion inhibition properties are often attributed to their phytochemical constituents (umoren and ebenso, 2008, Akalezi and Oguzie, 2015). The exploration of natural product of plant origin as ecofriendly, cost effective and non toxic sources of inhibitors for metal corrosion is an important field of research. Plants extracts especially those from the various parts of *citrus sinensis* (sweet orange) are extensively used in traditional medicine owing to their rich sources of secondary metabolites which have been found to have beneficial properties and form the basis for several important pharmaceutical drug formulations (Okafor *et al.*, 2008). *Citrus sinensis* is one of the most commonly consumed fruit all over the world as an excellent source of vitamin C which is a powerful antioxidant. Computational chemistry has been widely used to study reaction mechanisms and to interpret experimental results of compounds virtually (Kavitha *et al.*, 2017). However, literature is scanty on the use of ethanolic extract of *Citrus sinensis* as an inhibitor for the corrosion of aluminium in HNO<sub>3</sub>. Therefore, the objective of the present work is to investigate the corrosion inhibition behavior and mechanism of ethanolic extracts of *citrus sinensis* seed (CSS) on the corrosion of aluminium in Nitric acid medium by weight loss measurements and quantum studies.

### **Theoretical Underpinning**

Several theories have been adopted to explain the activities of the constituent of plant extracts on the metal/corrosion interface which among others include theories of reaction rate and the density functional theory (DFT).

### **Theories of Reaction Rate**

The general goal of theoretical chemical kinetics is to rationalize many of the empirical facts of chemical kinetics in terms of molecular properties. Prominent among these facts are the effects of concentration and temperature on reaction rates (Ibemesi, 2004). There are many theories involving reaction rate but this study is based on the Arrhenius Theory.

### **Effect of Temperature on Reaction Rate: Arrhenius Theory**

Increase of temperature generally increases the rate of a chemical reaction to a marked extent; as a rule of thumb, the specific rate constant of a homogeneous reaction is usually increased by a factor of about two to three for every 10<sup>0</sup> rise in temperature. An expression relating rate constant with temperature is given in equation 1.0.

$$\ln k = -\frac{E_a}{RT} + \ln A \quad 1.0$$

Where A is called the frequency factor or pre-exponential factor.

Okoronkwo *et al.*, (2015) in their study on the corrosion inhibition of mild steel in hydrochloric acid solution by the acid extract of *Gliricidia sepium* leaves observed that the corrosion rate generally increases in the absence of the inhibitor (blank) but decreases progressively with increased in concentration of the extract. They further pointed out that the inhibition efficiency of the plant extract decreases with increase in temperature from 303-323K.

### **Density functional Theory (DFT):**

The density functional theory (DFT) has been used to analyze the characteristics of the inhibitor/surface mechanism and to describe the structural nature of the inhibitor on the corrosion process (Ebenso *et al.*, 2010). The optical and electronic property of organic compounds is explained by analyzing their frontier molecular orbitals (FMO) like the highest occupied molecular orbital (HOMO) and lowest unoccupied molecular orbital (LUMO) (Obi-Egbedi *et al.*, 2011). The highest occupied molecular orbital (HOMO) is usually the region of high electron density, therefore is often associated with the electron donating ability of the molecule and lowest unoccupied molecular orbital (LUMO) is associated with the electron accepting ability of the inhibitor molecule from the metal. Hence, HOMO is the electron donating orbitals and LUMO is electron accepting orbitals (Singh *et al.*, 2017). In general for a good corrosion inhibitor HOMO value should be high, LUMO should be low and energy gap between the LUMO and HOMO ( $\Delta E$ ) should be low (Singh *et al.*, 2017).

According to Koopman's theorem the negative value of HOMO is related to the ionization potential (IE) whereas the negative value of LUMO correspond to the electron affinity (EA), as follows:

$$IE = -E_{\text{HOMO}} \quad 1.1$$

$$EA = -E_{\text{LUMO}} \quad 1.2$$

In literature, several DFT calculations are observed where inhibition efficiency and molecular structure/electronic properties of organic corrosion inhibitors have been correlated.

Akalezi and Oguzie, (2015) investigated the quantum parameters related to the molecular electronic structures of four predominant components of *Chrysophyllum albidum* (CS) extract. The result indicates that the constituent of CS extract are adsorb strongly on the iron surface and provide higher inhibition efficiency.

Zhang *et al.*, 2016 investigated the inhibition of methionine (Met) and proline (Pro) in PCMs solution using DFT and B3LYP/6-31G (d) method. The inhibition efficiency of Met and Pro follow the order of Met > Pro.

## **METHODOLOGY**

### **Collection of plant material and preparation of seed extracts**

The study was carried out on *Citrus sinensis* seeds (CSS). The *Citrus sinensis* seeds were collected from homes and street where the fruits were consumed locally by people around who discard the seed as waste in Okigwe local government area of Imo state, Nigeria. The sample was dried and grounded into powder. Four hundred and fifty gram

(450g) of the dehydrated and grounded seeds was soaked in a 500ml solution of ethanol for 48hrs. Sequentially, sufficient grams of the grounded seeds were measured into the ethanol and were extracted until the 450g of the grounded seeds were exhausted. After 48hrs, the samples were filtered using Whatman filter paper No.1 (QUALIGEN-Germany). The filtrates were further subjected to evaporation by rotatory evaporator at 358K in order to leave the sample free of the ethanol. The stock solutions of the extract obtained were used in preparing different concentrations of the extract by dissolving 0.2, 0.4, 0.6, 0.8 and 1.0g of the extract in 1L of 2M H<sub>2</sub>SO<sub>4</sub> acid respectively.

### **Chemical Analysis**

Screening of phytochemicals is significant for identification of bioactive principles present in plants. Phytochemical screening was carried out on CSS extracts by standard procedures (Khadom *et al.*, 2017). Plant extracts were screened for reducing sugar, alkaloids, protein, phenols, flavonoids, amino acids, tannin, steroids, glycosides and carbohydrates. These compounds are potential corrosion inhibitors for many metals in an acidic medium (Verma and Mehta, 1997)

### **Preparation of Specimen**

The specimens were cut using a saw into the required dimension of 4 x 3 x 0.035cm then descaled by brushing with a emery paper. They were cleaned and dried with acetone, then stored properly in desiccators for further use. The elemental composition of aluminium specimen were (wt %) Al(98.70), Si(0.48), Cl(0.014), K(0.04), Ca(0.01), Ti(0.005), V(0.016), Mn(0.012), Fe(0.50), Ni(0.013), Cu(0.048), Ga(0.013), In(0.10), Te(0.010), Ba(0.009), Os(0.032), and Ir(0.03). Mini pal, a compact energy dispersive X-ray spectrometer designed for the elemental analysis of a wide range of samples was used for the determination of the aluminium composition.

### **Gravimetric Techniques**

One hundred millilitres (100ml) each of the 1M HNO<sub>3</sub> solution was measured into six different beakers with one as the blank (uninhibited solution) and the remaining five labeled A to E containing different concentrations of the inhibitors ranging from 0.2g to 1.0g/100ml respectively. The test coupons were weighed before immersion in the acid solutions and the measurements were taken down. After weighing, the coupons were immersed in the acids solution. The coupon in each beaker was noted to avoid mix ups during the practical work. The immersion period was 2 hours interval, after 2 hours the coupons were retrieved from the acids, washed with tap water, degreased with ethanol and dried with acetone before the corresponding weights after immersion were recorded. The procedures were repeated for 8 hours. The corresponding weights after immersion were recorded as well after each 2 hours. The differences in weight of the coupons were again taken as the weight loss (Kavitha *et al.*, 2017). The rate of corrosion (CR), inhibition efficiency (IE), and degree of surface coverage ( $\Theta$ ) were obtained from the weight loss results.

The corrosion rates (C.R) were computed using the formular:

$$C.R = \frac{\Delta W}{A \times T} \quad 1.3$$

Where:  $\Delta W$  = weight loss (g),  $A$  = total surface area of the test coupon ( $\text{cm}^2$ ),  $T$  = immersion time (hrs)

The inhibitor efficiency (IE) was computed using the relationship in equation 1.4.

$$\%IE = \frac{(C.R)_o - (C.R)_{inh}}{(C.R)_o} \times 100 \quad 1.4$$

Where:  $(C.R)_o$  and  $(C.R)_{inh}$  are the corrosion rates in the absence and presence of different concentrations of the inhibitor, respectively.

The surface coverage ( $\theta$ ) of the inhibitor was obtained from the experimental data using the equation 1.5 as follows:

$$\theta = \frac{(C.R)_o - (C.R)_{inh}}{(C.R)_o} \quad 1.5$$

### **Fourier Transform Infrared Spectroscopy (FTIR) Analysis:**

FTIR analysis was used to ascertain the fact that the corrosion inhibition process takes place through the adsorption of the phytochemical constituents on the mild steel surface. The spectra of *CS* seed extract were recorded in a Perkin-Elmer-1600 spectrophotometer using KBr pellet.

### **Scanning Electron Microscopy (SEM) Analysis:**

The surface morphology of the mild steel before and after immersion were examined with scanning electron microscopy to analyse the elements on the surface, using a phenom pro X Scanning Electron Microscope (SEM). The electrons interact with atoms in the sample, producing various signals that can be detected and that contain information about the samples surface topography and composition.

### **Quantum Chemical Analysis:**

Quantum chemical calculations were used as a theoretical tool to support the experimental results and to explain the interaction between the inhibitor molecules and the steel surface. Density functional theory (DFT) was used to analyze the characteristics of the plant extracts and to describe the structural nature of the inhibitor on the corrosion process (Ebenso *et al.*, 2010, Obi-Egbedi *et al.*, 2011). Structures of flavonol and glucose as part of the components in *CS* seed extracts were obtained from literature for computational analysis. 3-Dimensional (3D) structures were retrieved from structural database and was optimized (Fig.3) and taken as input file for quantum chemical studies. The structures are sketched with ACD chemsketch. The calculated values of the quantum chemical parameters obtained using the Hartree-fock/ Density functional theory (HF-DFT) by Becke 3 Lee Yang Parr (B3LYP) method with 6-31G\* basis set of SPARTAN 06 V112 program are presented in Table 6.0. Mulliken population analysis determines nucleophilic and electrophilic reaction centers in compounds. Positive and negative regions in HOMO and LUMO orbitals, Mulliken charges, Electrostatic potential map of compounds were computed using ArgusLab 4.0.1 (Stewart, 2013, Thompson, 2004).

Other related parameters like electronegativity ( $\chi$ ), electronic chemical potential ( $\mu$ ), hardness ( $\eta$ ), and softness ( $\sigma$ ) can be expressed as:

$$\text{Electronegativity } (\chi): -\mu = \frac{IE+EA}{2}$$

1.6

$$\text{Electronic chemical potential } (\mu): -\chi \quad 1.7$$

$$\text{Hardness } (\eta): = \frac{IE-EA}{2} \quad 1.8$$

Electronegativity, hardness, and softness have proved to be very useful quantities in chemical reactivity theory.

The global electrophilicity ( $\omega$ ) index was introduced by Parr (1999) as a measure of energy lowering due to maximal electron flow between donor and acceptor and is given by

$$\text{Electrophilicity } (\omega): = \frac{\mu^2}{2} \sigma$$

1.9 Nucleophilicity ( $\varepsilon$ ): nucleophilicity is the reciprocal of electrophilicity expressed as:

$$\varepsilon = \frac{1}{\omega} \quad 2.0$$

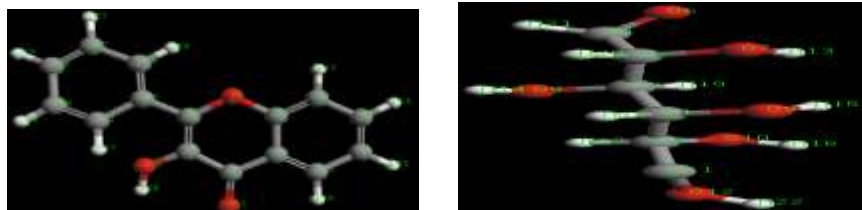


Figure 1.0: Optimized Structure of Flavonol and Glucose

## RESULTS

### Phytochemical Screening

The following phytochemicals were reported present in the CSS extract as well as their quantity;

**Table 1.0:** Phytochemical Constituent of CSS extract

Phytochemicals Constituent	CSS extract
Alkaoids	+
Saponin	+
Tannin	+++
Phenol	++
Flavonoid	++
Cardiac Glycoside	+
Steroid	+
Carbohydrates	+++
Proteins	+++
Amino Acids	++
Reducing Sugar	++

**Legend:** + = Sparingly Present; ++ = Moderately Present; +++ = Highly Present

**Corrosion Rate and Inhibitor Efficiency Results of CSS Extract**

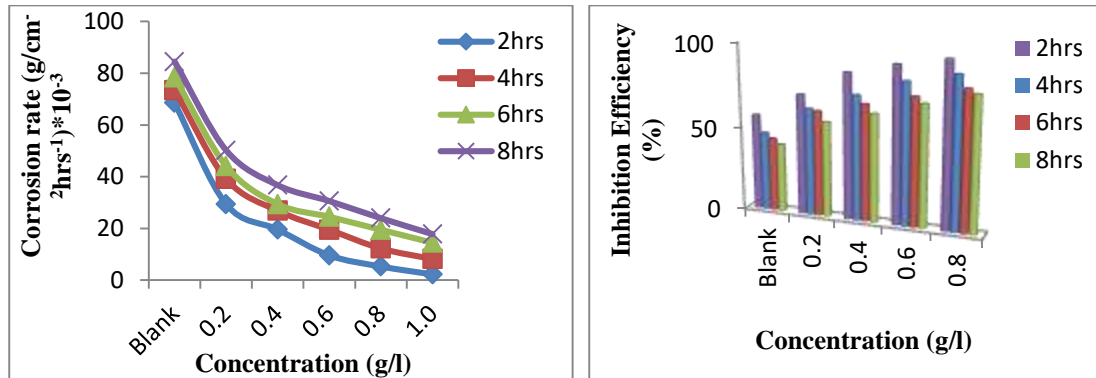


Figure 1.1: Variation of corrosion rate and inhibition efficiency with different Concentration of CSS extract for the corrosion of aluminium in 1M HNO<sub>3</sub> showing the effect of time.

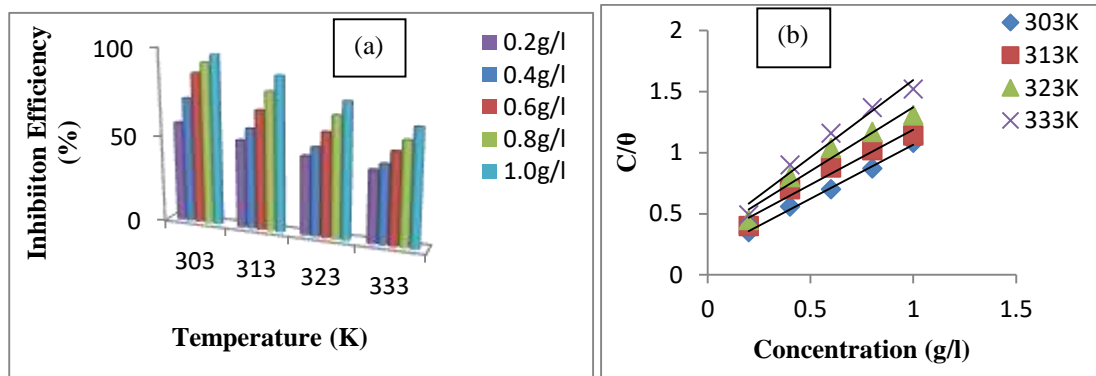


Figure 1.2: (a) Effect of temperature on inhibition efficiency for aluminium corrosion in 1M HNO<sub>3</sub> at different concentration of CSS extract (b) The Langmuir isotherm for the adsorption of CSS on aluminium surface in 1M HNO<sub>3</sub>.

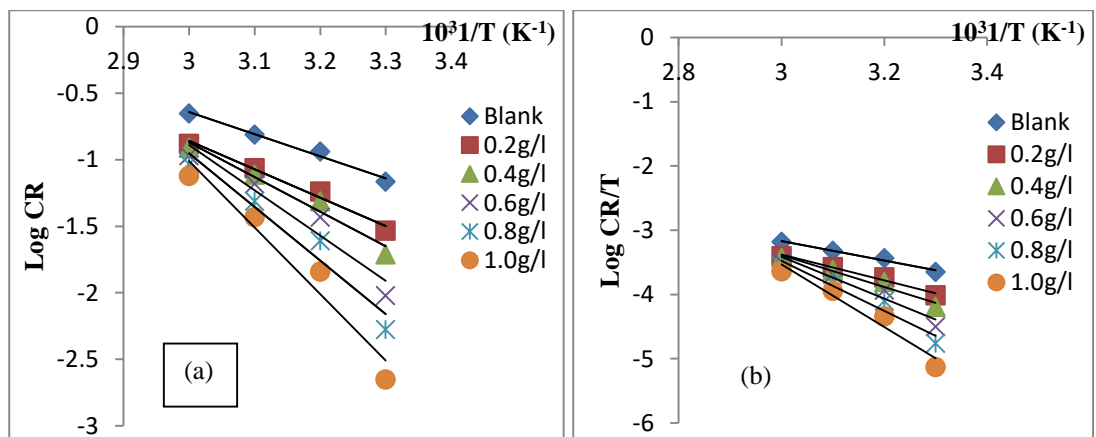


Figure 1.3: (a) Plot of log CR against 1/T and (b) Plot of CR/T against 1/T for aluminium in 1M HNO<sub>3</sub> solution in the absence and presence of various concentrations of inhibitor.

Table 2: corrosion rate (CR) and inhibition efficiency (I.E) for aluminium corrosion in different concentration of HNO<sub>3</sub> solution in the presence and absence of CSS extract for 2h.

Inhibitor Concentration (g/l)	Acid Concentration					
	1.0M		1.5M		2.0M	
	CR (gcm <sup>-2</sup> h <sup>-1</sup> ) x 10 <sup>-3</sup>	I.E (%)	CR (gcm <sup>-2</sup> h <sup>-1</sup> ) x 10 <sup>-3</sup>	I.E (%)	CR (gcm <sup>-2</sup> h <sup>-1</sup> ) x 10 <sup>-3</sup>	I.E (%)
Blank	68.60	-----	71.50	-----	77.04	-----
0.2	29.40	57.14	37.16	48.03	42.74	44.52
0.4	19.60	71.43	24.91	65.20	28.04	63.60
0.6	9.60	86.00	17.56	75.44	23.14	70.00
0.8	5.31	92.26	11.23	84.30	18.31	76.23
1.0	2.25	96.72	8.17	88.57	13.27	82.78

Table 3: Calculated values of corrosion rate for aluminium in 1M HNO<sub>3</sub> in the absence and presence of CSS at 303–333K.

Concentration of the extract (g/l)	Corrosion Rate (gcm <sup>-2</sup> h <sup>-1</sup> ) x 10 <sup>-3</sup>			
	303K	313K	323K	333K
Blank	68.60	115.51	156.77	222.77
0.2	29.40	57.76	86.63	132.01
0.4	19.60	49.51	78.38	123.76
0.6	9.60	37.13	66.01	107.26
0.8	5.31	24.75	49.51	92.82
1.0	2.25	14.44	37.13	76.32

Table 4: Adsorption parameters for the adsorption of ethanolic extract *C. sinensis* seed on the surface of aluminium in HNO<sub>3</sub>.

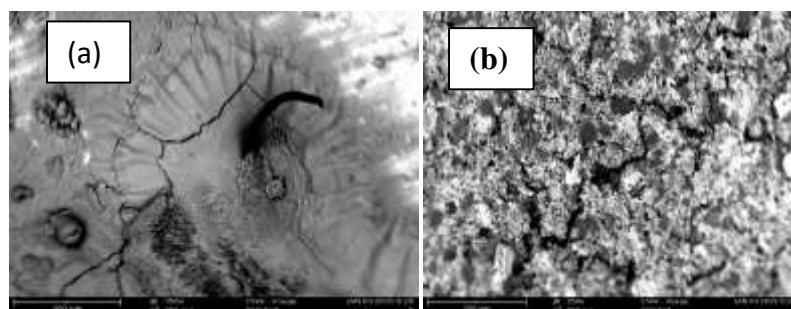
Isotherm	Temperature (K)	K <sub>ads</sub>	ΔG <sub>ads</sub> (KJmol <sup>-1</sup> )	R <sup>2</sup>
Langmuir	303	5.53	-14.43	0.995
	313	3.47	-13.69	0.962
	323	3.06	-13.79	0.952
	333	3.04	-14.20	0.963
Freundlich	303	1.04	-10.22	0.985
	313	0.84	-10.00	0.952
	323	0.73	-9.94	0.935
	333	0.62	-9.80	0.921

Table 5: Energy parameters for the dissolution of aluminium in HNO<sub>3</sub> in the absence and presence of different concentrations of *C. sinensis* seed extract.

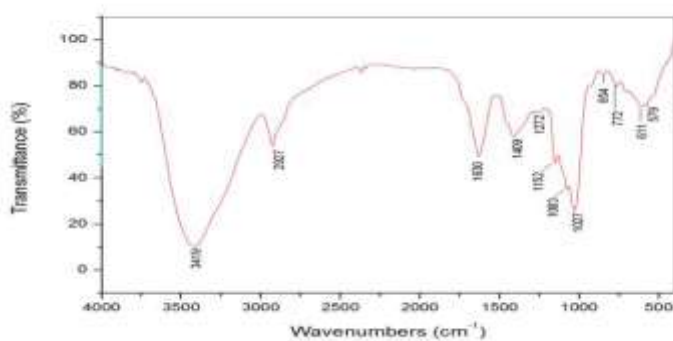
Inhibitor Concentration (g/l)	$\Delta E_a$ (KJmol <sup>-1</sup> )	$\Delta H_a$ (KJmol <sup>-1</sup> K <sup>-1</sup> )	$\Delta S_a$ (KJmol <sup>-1</sup> )	$Q_{ads}$ (KJmol <sup>-1</sup> ) 303-313K
Blank	31.85	29.17	-0.171	-----
0.2	40.83	38.20	-0.148	-22.56
0.4	49.79	47.13	-0.121	-49.60
0.6	65.11	62.51	-0.076	-84.09
0.8	77.16	74.34	-0.041	-93.35
1.0	95.75	93.26	-0.005	-47.04

Table 6.0: Quantum Chemical Parameters of CSS Phytoconstituents

Component Parameters	Flavonol	Glucose
$E_{HOMO}$ (eV)	-0.3301	-0.2896
$E_{LUMO}$ (eV)	-0.0370	-0.0153
$\Delta E_{(LUMO-HOMO)}$ (eV)	0.2931	0.2743
$EA$ (eV)	0.0370	0.0153
$IE$ (eV)	0.3301	0.2896
$\chi$ (eV)	0.1836	0.1525
$\eta$ (eV)	0.1466	0.1372
$\sigma$ (eV <sup>-1</sup> )	6.8213	7.2886
$\omega$ (eV)	0.1150	0.0875
$\epsilon$ (eV)	8.6957	11.4286
$\mu$ (debye)	1.7189	5.0326



**Figure 1.4:** (a) SEM of the mild steel immersed in 1M HNO<sub>3</sub> solution without inhibitor for 5 hrs at 200 magnification and (b) SEM of the mild steel immersed in 1M HNO<sub>3</sub> solution in the presence of CS seed extract.



**Figure 1.5:** FTIR spectra of *Citrus sinensis* seed extract (CSSE)

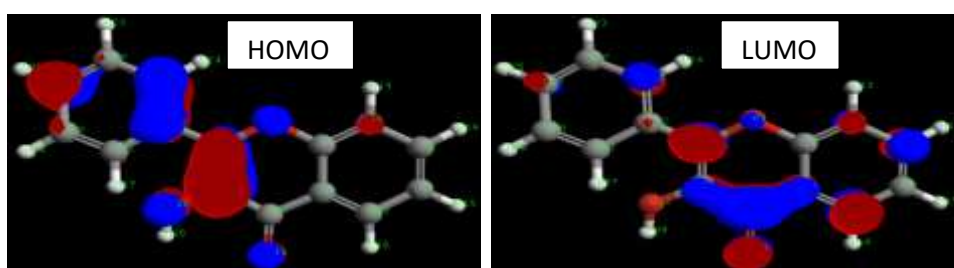


**Figure 1.6:** HOMO and LUMO orbitals of Flavonol

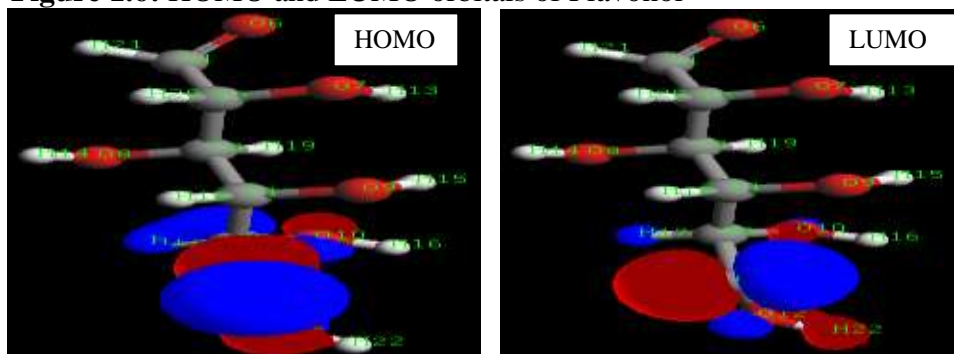


**Figure 1.7:** HOMO and LUMO orbitals of Glucose

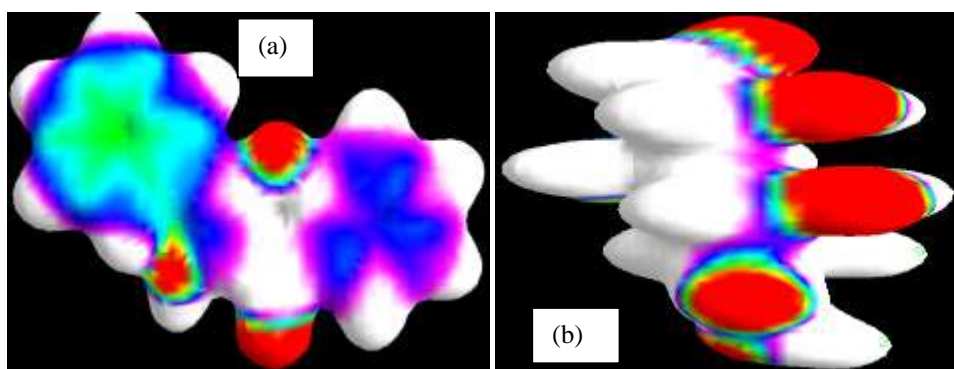


**Figure 2.2:** ESP Optimized mapped density of (a) Flavonol and (b) Glucose

Table 7.0: Mulliken Charge Distribution on Flavonol, alkaloid and Arginine

Atomic Charges on Flavonol		Atomic Charges on Alkaloid	
1	O -0.1185	1	C -0.6588
2	C 0.0993	2	C -0.2075
3	C -0.2138	3	C -0.5098
4	C 0.3705	4	C -1.1775
5	C -0.0914	5	C -1.1045
6	C 0.0929	6	O 0.0901
7	C -0.2413	7	O 1.3320
8	C -0.1319	8	O 0.5692
9	C -0.2373	9	O 0.7259
10	C -0.0735	10	O 2.4463
11	O -0.3576	11	C -1.1735
12	O -0.2357	12	O 0.4586
13	H 0.2185	13	H -0.2523
14	H 0.2001	14	H 0.1795
15	H 0.2067	15	H -0.1073
16	H 0.2251	16	H -1.0308
17	C -0.2013	17	H 0.0232
18	C -0.1620	18	H 0.8150
19	C -0.1807	19	H -0.3410
20	C -0.2000	20	H -0.2114
21	C -0.2243	21	H -0.0869
22	C -0.0540	22	H 0.2217
23	H 0.1951		
24	H 0.2070		
25	H 0.1917		
26	H 0.1947		
27	H 0.2967		
28	H 0.2250		

## DISCUSSION

### Gravimetric measurement

Figure 1.1, shows the plot of Variation of corrosion rate and inhibition efficiency with different Concentration of *Citrus sinensis* seed extract for the corrosion of aluminium in nitric acid as a function of time. The addition of various concentrations of CSS reduced the dissolution of the metal into the acid medium. This could be as a result of the adsorption of the extract constituents covering the surface of the mild steel, thereby retarding the rapid dissolution of the coupons. From the plot, the corrosion rate increased with an increase in immersion time but decreased with an increase in inhibitor concentration. It was observed that there is a significant reduction in corrosion rate of the aluminium immersed in the solution of the acid containing CSS. The commutative corrosion rate of the metal in the absence of CSS at the end of the 8th hour was  $0.008452\text{gcm}^{-2}\text{h}^{-1}$ , while in the presence of 1.0g/l CSS the corrosion rate reduced to  $0.001786\text{gcm}^{-2}\text{h}^{-1}$ . This also is in tandem with what was observed in the inhibitory

action of *Momordica charantia* seed extracts on the corrosion of mild steel (Kavitha *et al.*, 2017).

The inhibition efficiency increased with increase in concentration of inhibitor from 0.2 to 1.0g/l at 303K (Fig.1.3). Maximum inhibition efficiency was 96.72% in case of CSS /1MHNO<sub>3</sub> for immersion period of 2h at a concentration of 1.0g/l (Fig.1.1). These results suggest that adsorption model arrangement and orientation of constituents present in *Citrus sinensis* seed extract on the surface of mild steel may change with time (Rekha *et al.*, 2010). Decrease in inhibition efficiency thereafter with increasing time may be due to shift in adsorption and desorption equilibria which takes place simultaneously on prolonged exposure to corrosive media ( Kavitha *et al.*, 2016). Adsorbed organic molecules prevent further interaction of metal with acid (Lahodny-Sarc and Kapor, 2002). The results obtain from table 2 indicates that when the acid concentration increases, corrosion rate increase and inhibition efficiency decrease.

### **Effects of temperature on inhibition efficiency and corrosion rate**

The effect of temperature on inhibition efficiency and corrosion rate was studied at the temperature range of 303 – 333K. The variation of inhibition efficiency with temperatures at different concentration of the CSS extract is shown in Figure 1.2 (a). From the plot, the inhibition efficiency increases with an increase in CSS extract concentration but decreases with an increase in temperature.

According to Alinor and Ejimeke (2012), at higher temperatures, the average kinetic energy of components of extracts increases, thus making adsorption between components of extracts and a metal surface insufficient to retain the species at the binding site and this could lead to desorption or cause the species to bounce off the surface of the metal instead of colliding and combining with it. Moreover, the solubility of the protective films on the metal surface would have occurred at a higher temperature, hereby exposing the metal surface to the aggressive medium, leading to more dissolution at this temperature.

The values of the corrosion rate at different temperatures are summarised in Table 3. It is clear from the table that the corrosion rate increases with a rise in temperature. This happened to be the case because, as the temperature increases, the average kinetic energy of the reactant molecules increases, thereby increasing the rate of the reaction. A decrease in inhibition efficiency with a rise in temperature and a corresponding increase in activation energy (E<sub>a</sub>) in the presence of an inhibitor is termed physical adsorption mechanism (Ebenso *et al.*, 2008).

The corrosion rate values were used to evaluate the activation energy and using transition state equation 2.1. The Plot of log CR as a function of reciprocal of absolute temperature, 1/T in the absence and presence of CSS extract as shown in Figure 1.3a gives a straight line with slope equal to  $-E_a/2.303R$ , from which the activation energy for the corrosion process can be calculated.

$$\log CR = \log A - \frac{E_a}{2.303RT} \quad 2.1$$

$$\log CR/T = \{ \log R/N_A h + \Delta S_a / 2.303 \} - \Delta H_a / 2.303 RT \quad 2.2$$

where CR is the corrosion rate,  $E_a$  is the apparent activation energy, R is the molar gas constant, T is the absolute temperature and A is the Arrhenius or frequency factor. The adsorption of the component of CSS extract on the surface of aluminium, increases the activation energy of the metal dissolution. In a chemical reaction, when the activation energy increases, the rate of the reaction decreases (Okoronkwo *et al.*, 2016). This is also seen in the results shown in Table 5; the addition of the inhibitor increases  $E_a$ , thereby reducing the rate of the metal dissolution into the electrolyte.

Plot of  $\log CR/T$  as a function of  $1/T$  from Equation (6), as shown in Figure 1.3b gives a straight line with slope equal to  $-\Delta H_a / 2.303R$  and intercept of  $\{ \log R/N_A h + \Delta S_a / 2.303R \}$ , from which the enthalpy and entropy of activation for the corrosion process can be calculated. Values of  $E_a$ ,  $\Delta S_a$ , and  $\Delta H_a$  are presented in Table 5.

The heat of adsorption ( $Q_{ads}$ ) of ethanolic extract of CS seed on the surface of aluminium has been calculated using equation 2.3 (Ebenso, 2003a, b, 2010; Umoren *et al.*, 2006a, 2006b, 2007).

$$Q_{ads} = 2.303R \left( \log \left[ \frac{\theta_2}{1-\theta_2} \right] - \log \left[ \frac{\theta_1}{1-\theta_1} \right] \right) \times \left[ \frac{T_1 T_2}{T_2 - T_1} \right] \quad 2.3$$

Values of  $Q_{ads}$  calculated through equation 2.3 are recorded in Table 5. These values are negative and ranged from -22.56 to -93.35 KJ/mol indicating that the adsorption of the extract is exothermic (Ebenso, 2003a, b, 2010; Bhajiwala and Vashi, 2001).

It is evident from Table 5 that the enthalpies of activation of the corrosion process are positive which reflect the endothermic nature of the dissolution process. The entropy of activation in the presence and absence of the inhibitor also has negative values which indicate that the activated complex in the rate-determining step represents an association, rather than dissociation, meaning that a decrease in disordering took place when going from the reactant to the activated complex (Lebrini, Robert, & Roos, 2011, Awe *et al.*, 2015).

### Adsorption isotherm

The adsorption mechanism of phytochemical constituents on a metal surface can be explained in terms of adsorption isotherm. In this study, results obtained for the degree of surface coverage at all temperatures were fitted to a series of different adsorption isotherms. Assumptions of Langmuir adsorption isotherm is expressed in equation 2.4 below (Shockry *et al.*, 1998):

$$C/\theta = 1/k + C \quad 2.4$$

Figure 1.2b shows the Langmuir adsorption isotherm for the plant extracts; from the result, values of  $R^2$  were very high close to unity, indicating a high degree of fitness adsorption data to the model. The tests revealed that the Langmuir adsorption model best described the adsorption characteristics of the studied plant extract. It is also significant to note that the value of the adsorption equilibrium constant obtained from

the intercept of each adsorption isotherm as shown in table 4, is related to the free energy of adsorption according to the equation.

$$\Delta G^{\circ}_{ads} = - RT \ln(55.5K_{ads})$$

2.5

The standard Gibbs free energy calculated for the two adsorption isotherms at various temperatures for the plant extracts is also presented in Table 4; from the results obtained, the free energies are found to be negatively less than the threshold value of  $-40 \text{ kJ mol}^{-1}$  required for the mechanism of chemical adsorption to take place. Therefore, the adsorption of the studied plant extracts on both aluminum and mild steel surface is spontaneous and is consistent with the mechanism of physical adsorption (Lebrini, *et al.*, 2010; Loto, 2011; Singh *et al.*, 2010, Okoronkwo *et al.*, 2015).

### Surface Studies by Scanning Electron Microscopy

Morphological analysis using SEM shows differences in the morphologies of the samples in the uninhibited and inhibited medium. Figure 1.4 showed the SEM image of the mild steel surface immersed in the uninhibited medium for 4 hours, big pits and cracks observed in the image are due to the effect of corrosion on the specimen infused by the acid. Similar image of mild steel immersed in the inhibited medium are also shown in Figure 1.4, Smother surfaces with little cracks observed are due to the formation of a thin film layer infused by the complexation between the mild steel and the phyto- chemical constituents in the extract. This implies corrosion rate was lowered by the extract which is in agreement with the results obtained from the weight loss analysis.

### Infrared Spectroscopy Analysis

FTIR analysis is used to ascertain the fact that the corrosion inhibition process takes place through the adsorption of the phytochemical constituents on the mild steel surface. The spectra of the extract are presented in figure 1.8. from the result obtained, the strong and broad peak of O-H stretching that obscured the appearance of other peaks basically N-H peak occurs at  $3419 \text{ cm}^{-1}$  with C-H stretching vibration occurring at  $2927 \text{ cm}^{-1}$ . The strong band at  $1630 \text{ cm}^{-1}$  is assigned to C=C and C=O stretching vibration. Owing to the conjugation effect of flavonoids of *BE* seed extract, the C=O peak shifts from about  $1700 \text{ cm}^{-1}$  to lower wave number (approximately  $1630 \text{ cm}^{-1}$ ), C=C and C=O stretching vibration bands are superposition (Deng *et al.*, 2007). The C-H bending bands in  $-\text{CH}_2$  and  $-\text{CH}_3$  are found to be at  $1409 \text{ cm}^{-1}$ . The absorption bands at  $1272 \text{ cm}^{-1}$  could be assigned to the framework vibration of aromatic ring. The IR spectra of the extracts showed peaks attributed to the characteristics of the functional groups. The presence of these functional groups indicates the effectiveness of the extract constituents to interact with the mild steel surface and that adsorption between the extract and the mild steel occurs through the identified functional groups (Okoronkwo *et al.*, 2015). Hence, protection of metallic surface is done via the functional groups presented in the flavonoids, tannin, carbohydrates, alkaloid and amino acids as the main constituents of *Citrus sinensis* seed extracts.

### Theoretical and Quantum Chemical Studies

Flavonol, and Glucose represent the most effective component of the *BE* seed extract. Quantum chemical calculations have proved to be a veritable tool for studying

corrosion inhibition mechanism (Kalaiselvi *et al.*, 2014, Khadom *et al.*, 2016). Thus in the present investigation, quantum chemical calculation were performed using density functional theory (DFT) to explain the experimental results obtained in this study and to give an insight into the inhibition action of the *BE* seed extract on the mild steel surface. The relation between inhibition efficiency of inhibitor and the quantum chemical calculation parameters like  $E_{\text{HOMO}}$ ,  $E_{\text{LUMO}}$ ,  $\Delta E$ ,  $\chi$ ,  $\eta$ ,  $\sigma$ ,  $\omega$ ,  $\varepsilon$ , and dipole moment were investigated (Table 6). In this study, the optimized geometry of the components of *CS* seed extract is shown in Figure 1.0. The positive and negative phases of orbital are represented by two colours, blue regions represent an increase in electron density and red region represents a decrease in electron density (K. Laxmi, 2014).

The Positive and negative regions in HOMO and LUMO orbitals of flavonol and glucose components of *CS* seed extract were plotted and are shown in Figure 1.6-1.7 respectively. From the Figure 1.6-1.7, It can be seen that the frontier orbitals, the HOMO and the LUMO were distributed all around each molecule most dominated by bonded heteroatoms (oxygen atoms of both hydroxyl and carboxylic group) and some of the carbon atoms basically those containing unsaturated bonds in their molecule, and on the entire aromatic rings. These regions are the sites at which electrophiles attack and represent the active centers, with the utmost ability to bond to the metal surface, whereas the LUMO orbital can accept the electrons in the d-orbital of the metal using antibonding orbitals to form feedback bonds (Martinez and Tagljar, 2003, Khaled, 2010). It has been reported that excellent corrosion inhibitors are usually those organic compounds that does not only offer electrons to unoccupied orbital of the metal but also accept free electrons from the metal (Soltani *et al.*, 2012). It is also well documented in literature that the higher the HOMO energy of the inhibitor, the greater its ability of offering electrons to unoccupied d-orbital of the metal, and the higher the corrosion inhibition efficiency. It is evident from Table 6.0 that flavonol had the highest value of  $E_{\text{HOMO}}$  -0.3302 (ev) and increased in the order: Fla>Glu which suggest that flavonol would be better adsorbed on the metal surface than glucose.  $E_{\text{LUMO}}$  represent the ability of the molecule to accept electrons from a donor reagent and the lower the value of  $E_{\text{LUMO}}$ , the greater the tendency of the molecule to accept electrons. Results from Table 6.0 also show that glucose had the lowest value of  $E_{\text{LUMO}}$  -0.0153 (ev) and decreases in the order: Glu<Fla which suggest that glucose will readily accept electron from the metal than flavonol. The above assertion indicate that *CS* seed extract is a good corrosion inhibitor capable of donating electrons to the aluminium surface, by forming an inhibition barrier (I.B. Obot *et al.*, 2015). This also confirms that the presence of this component molecules in the seed extract increases its inhibition efficiency which is in line with the experimental results.

Apart from  $E_{\text{HOMO}}$  and  $E_{\text{LUMO}}$ , energy gap ( $\Delta E = E_{\text{LUMO}} - E_{\text{HOMO}}$ ) is another essential quantum chemical parameter for explaining surface adsorptive behaviour of the inhibitor molecules. Generally, Larger value of  $\Delta E$  implies that the inhibition efficiency of the inhibitor is less due to low reactivity with the metal surface and lower value of  $\Delta E$  implies that the inhibitor is having higher inhibition efficiency due to high reactivity with metal surface. Low values of the energy gap ( $\Delta E$ ) will provide good inhibition efficiencies, because the excitation energy to remove an electron from the last occupied orbital will be low (Gece, 2008). A molecule with a low energy gap is more polarizable and is generally associated with a high chemical reactivity, low kinetic stability and is

termed soft molecule (Dwivedi and Misra, 2010). In this study, Table 6.0 shows the lower values of  $\Delta E_{(LUMO-HOMO)}$  in the following order Flavonol (0.2931) < Glucose (0.2743). The adsorption of inhibitor onto a metallic surface occurs at the part of the molecule which has the greatest softness and lowest hardness (Wang, 2012).

Chemical hardness ( $\eta$ ) and softness ( $\sigma$ ) are significantly related to the band gap (HLG). They are important properties to measure the stability and reactivity of a molecule. A soft molecule has a small energy gap and a hard molecule has a large energy gap (Obi-Egbedi *et al.*, 2011). According to Pearson, hard molecules with large energy gaps cannot act as good corrosion inhibitors. Conversely, soft molecules with small energy gaps are efficient corrosion inhibitors because they can easily donate electrons to metal atoms at the surface. Table 6.0 reveal that constituent of CS seed extract have greater values of softness ( $\sigma$ ) and lower values of hardness ( $\eta$ ). The CS seed ( $\sigma$ ) values of the studied extract increases in the order: Glucose (7.2866) > Flavonol (6.8213) and the corresponding hardness values decreases in the reverse form of the order: Glucose (0.1372) < Flavonol (0.1466). This confirmed the extract molecule as efficient corrosion inhibitor

Moreover the mapping of molecular electrostatic potential (ESP) can allow an observation of the regions of high and low electron density in an organic corrosion inhibitor molecule. This can help determine the possible sites in the inhibitor molecule which are susceptible to undergo adsorption interaction with a metal surface (Dohare *et al.*, 2017, Haque *et al.*, 2017a). The ESP mapping of the Component of CS seed extract are displayed in Figure 1.8. The different values of ESP are shown in different colours where the most negative ESP regions are shown in red colour i.e. regions rich in electron, blue colour shows the region of the most positive ESP that is electron deficiency while the green colour shows the regions with zero ESP values (Haque *et al.*, 2017b, Chauhan *et al.*, 2018). It can be seen that in the Component of CS seed extract, the most negative potential (red color) is around the heteroatoms (oxygen and nitrogen). Upon protonation at nitrogen, a deep blue coloured region can be observed around the nitrogen atoms showing a deficiency of electrons and the possible centre's susceptible for undergoing physical adsorption via electrostatic interaction.

### **Mulliken charge distribution of Flavonol and Glucose**

Mulliken population analysis is mostly used for calculation of charge distribution in a molecule (S. Martinez and I. Tagljar, 2003). Mulliken charge distribution of flavonol and alkaloid are presented in Table 7.0. It shows Mulliken charge distribution of all heteroatoms and some of carbon atoms are negatively charged. Thus, considered as active sites for adsorption process of inhibitor molecule onto the aluminium surface (Lgaz *et al.*, 2016). More negative the atomic charges of adsorbed centre, more easily atom donates its electron to unoccupied orbital of the metal (Musa *et al.*, 2010). The inhibition efficiency of inhibitors under study depends on presence of electronegative atoms in their molecular structure. It can be readily observed that oxygen atoms and most of the carbon atoms have higher charge densities/negative charges. Glucose has more electronegative C1 and C3 with charges -0.6588 and -0.5098. In glucose, C1, C3, C2, and C4 are most susceptible sites for electrophilic attacks as they present highest values of negative charge. On other hand, O9, O8 and O12 in glucose are the most susceptible sites for the nucleophilic attacks as they present the highest values of

positive charge were active centers that possess strong ability of bonding to metal surface occur. The regions of highest electron density are generally sites to which electrophiles can attack (Musa *et al.*, 2010). Flavonol has C21, C9, C7, O11 and O12 as the most susceptible sites for electrophilic attacks as they offer the highest values of negative charge. However, C4 in Flavonol is the most susceptible sites for the nucleophilic attacks as its present the highest values of positive charge. Therefore Glucose and Flavonol can accept electrons from metal through these atoms and hence these compounds could serve as good corrosion inhibitor against metal surface protection.

### **Implication to Research and Practice**

The study provides information on the use of ethanol extract of *Citrus sinensis* as a corrosion inhibitor. Electrochemical studies such as polarization and alternating current impedance spectra will throw more light on the mechanistic aspects of the corrosion inhibition. This environmentally friendly inhibitor could find possible applications in metal surface anodizing and surface coatings.

### **CONCLUSION**

From the above results and discussions, the following conclusion was drawn:

- ❖ All the studied phytochemical constituent of the seed extracts acts as an effective corrosion inhibitor of mild steel in 1M HNO<sub>3</sub> acid solution and their inhibition efficiency increases with increase in the concentration of the seed extracts with maximum efficiency obtained at an optimum concentration of 1.0g/l within the first 2 hours.
- ❖ The adsorption data was best fitted into Langmuir adsorption models.
- ❖ The results of SEM and Fourier transform infrared spectroscopy (FTIR) all indicate that the corrosion reaction was inhibited by the adsorption of the extract's organic matter onto the corroding mild steel surface.
- ❖ The trends of inhibition efficiency with temperature and activation parameters for corrosion and corrosion inhibition processes point toward significant physisorption of the extract constituents on the aluminium surface.
- ❖ DFT-based quantum chemical computation was used to theoretically model the physisorptive interactions between the plant extract's molecules, which are the active components of the extract and mild steel surface. The magnitude of the obtained adsorption energy confirms strong physisorption of the molecules.
- ❖ Phytochemical screening, weight loss measurements, and quantum analysis confirmed the corrosion preventive property of *Citrus sinensis* seed (CSS) in 1M HNO<sub>3</sub> medium. The investigation shows *Citrus sinensis* seed (CSS) extract as an excellent inhibitor for aluminium corrosion in 1M HNO<sub>3</sub>.

### **Future Research**

1. Constraint in the availability of equipment has subjected this research to weight loss methods and Computational/Quantum analysis however, subsequent investigation can be carried out using A.C impedance and linear polarization methods for comparison.

2. The effects of the extracts on the corrosion of other metals like mild steel, copper, zinc e.t.c at various temperatures could be investigated.
3. Mediums such as H<sub>2</sub>SO<sub>4</sub>, HCl etc could be use to characterized the inhibition propensity of these inhibitors

### **Acknowledgement**

The authors expresses their profound gratitude to Dr. Kufre for his technical advice and help in Quantum analysis of the extract. Also we sincerely thanks the other staffs of the department of chemistry Akwa Ibom State University for their support in providing the enabling environment for the lab work.

### **Reference**

- Akalezi C.O and Oguzie E.E (2015). Evaluation of anticorrosion properties of chrysophyllum albdum leaves extract for mild steel protection in acidic media. *International Journal of Industrial Chemistry*, 7:81-92
- Alinnor I. J and Ejikeme P.M, (2012). Corrosion Inhibition of Aluminium in Acidic Medium by Different Extracts of Ocimum Gratissimum, *American Chemical Science Journal*. 2(4), 122-135.
- Awe F.E, Idris S.O, Abdulwahab M, and Oguzie EE, (2015). Theoretical and experimental inhibitive properties of mild steel in HCl by ethanolic extract of *Boscia senegalensis*. *Cogent Chemistry* ,1:1112676. dx. Doi . org /10.1080/23312009.1112676
- Banu V.N, Rajendran S. and Kumaran S.S. (2016). *J. Alloys Compd.*, 675, 139–148.
- Bammou L, Belkhaouda M, Salghi R, Benali O, Zarrouk A, Zarrok H and Hammouti B, (2014). Corrosion inhibition of steel in sulfuric acidic solution by chenopodium ambrosioides extract. *J. Asso. Arab. Uni. Basic. Appl. Sci.*, Vol. 16: 83 – 90,
- Bhajiwala HM, Vashi RT (2001). Ethanolamine, diethanolamine and triethanolmine as corrosion inhibitors for zinc in binary acid mixture (HNO<sub>3</sub> + H<sub>3</sub>PO<sub>4</sub>). *Bull. Electrochem*, 17: 441– 448.
- Chauhan D.S, Srivastava V, Joshi P.G, Quraishi M.A. (2018). PEG cross-linked Chitosan: a biomacromolecule as corrosion inhibitor for sugar industry. *International Journal of Industrial Chemistry.*, <https://doi.org/10.1007/s40090-018-0165-0>
- Dohare P, Chauhan D, Sorour A, Quraishi M. (2017). DFT and experimental studies on the inhibition potentials of expired Tramadol drug on mild steel corrosion in hydrochloric acid. *Mater Discov* 9:30–41
- Deng Q.Y., Liu L. and Deng H.M, (2007). *Principles of Spectrometric Identification*, 2nd Edition, Science Press, Beijing, p. 37.
- Dwivedi A and Misra N, 2010. *Der pharma. Chem.* 2, 58. EL Basiony N.M, Elgendy Amr, Nady H, Migahed M.A, and Zaki EG, (2019). Adsorption characteristics and inhibition effect of two Schiff base compounds on corrosion of mild steelin 0.5 M HCl solution. *RSC Adv.*, 9, 10473
- Ebenso E.E. (2003a). Synergistic effect of halide ions on the corrosion inhibition of aluminium in H<sub>2</sub>SO<sub>4</sub> using 2-acetylphenothiazine. *Mater. Chem. & Phys.* 79: 58-70.
- Ebenso E.E. (2003b). Effect of halide ions on the corrosion inhibition of mild steel in H<sub>2</sub>SO<sub>4</sub> using methyl red. Part 1, *Bull Electrochem.* 19:209 – 216.

- Ebenso E.E, Isabirye D.A and Eddy N.O, (2010). Adsorption and Quantum Chemical Studies on the Inhibition Potentials of Some Thiosemicarbazides for the Corrosion of Mild Steel in Acidic Medium, *Int. J. Mol. Sci.*, Vol. 11, No. 6, pp. 2473-2498,
- Ebenso E.E, Eddy N.O and Odiongenyi A.O., (2008). Corrosion inhibitive properties and adsorption behaviour of ethanol extract of *Piper guinensis* as a green corrosion inhibitor for mild steel in H<sub>2</sub>SO<sub>4</sub>. *African Journal of Pure and Applied Chemistry*. 2 (11): 107-115
- Gutierrez E, Rodr'iguez JA, Cruz-Borbolla J, Alvarado-Rodr'iguez JG and Thangarasu P, (2016), *Corros. Sci.*, 108, 23–35.
- Gece G. (2008). The use of quantum chemical methods in corrosion inhibitor studies. *Corros Sci* 50:2981–2992. <https://doi.org/10.1016/j.corsci.2008.08.043>
- Haque J, Ansari K, Srivastava V, Quraishi M, Obot I, 2017a. Pyrimidine derivatives as novel acidizing corrosion inhibitors for N80 steel useful for petroleum industry: a combined experimental and theoretical approach. *J Ind Eng Chem* 49:176–188,
- Haque J, Srivastava V, Verma C, Quraishi M, 2017b. Experimental and quantum chemical analysis of 2-amino-3-((4-((S)-2-amino-2-carboxyethyl)-1H-imidazol-2-yl)thio) propionic acid as new and green corrosion inhibitor for mild steel in 1 M hydrochloric acid solution. *J Mol Liq* 225:848–855
- Ibemesi, J. A. (2004). Physical chemistry for tertiary institution, part 1. 2nd edition. Nsukka: Fijac Academic Press.
- Junaedi S, Kadhum AH, Al-Amiery AA, and Muhamad A 2012. Synthesis and characterization of novel corrosion inhibitor derived from oleic acid: 2-Amino 5-oleyl-1,3,4-thiadiazol (AOT). *Int. J. Electrochem. Sci.*, 7, 3543- 3554
- James A.O and Akaranta O, (2009). Corrosion inhibition of aluminum in 2.0 M hydrochloric acid solution by the acetone extract of red onion skin. *African Journal of Pure and Applied Chemistry* Vol. 3 (12), pp. 262-268
- Khaled, K.F. (2010). Corrosion control of copper in nitric acid solutions using some amino acids – A combined experimental and theoretical study. *Corrosion Science*, 52, 3225–3234.
- Kavitha V. and Gunavathy N., (2016). Theoretical Studies on Corrosion Inhibition Effect of Coumarin and its Derivatives against Metals using Computational Methods, *International Journal of Engineering and Technique*, 2(6): 2395-1303
- Kavitha V, Gunavathy N, Poovarasi S (2017). Efficacy of Seed Extracts of *Momordica Charantia* on the Corrosion Inhibition of Mild Steel in 1N HCl Medium using Phytochemical Screening, Weight loss Measurements and Quantum Chemical Studies, *IJARIE3* (4): 2395-4396
- Kalaiselvi K, Brindhya T and Mallika J, (2014). “Quantum Chemical Studies on the Corrosion Inhibition of Mild Steel by Piperidin-4-One Derivatives in 1 M H<sub>3</sub>PO<sub>4</sub>,” *O. J. metal*, vol. 4, 73-85,
- Khadom, AA, Karim HH and Noor HK, (2016). Quantum Chemical study of *Citrus aurantium* leaves extracts as a sustainable corrosion inhibitor of mild steel in sulfuric acid. *Australian Journal of Basic and Applied Sciences*, 10(15) 127-133,
- Khadom A.A, Abd A.N, Ahmed N.A, (2017). *Xanthium strumarium* leaves extracts as a friendly corrosion inhibitor of low carbon steel in hydrochloric acid: kinetics and mathematical studies. *SAJCE* 25:13–21

- Lgaz R., Salghi M, Larouj M, Elfaydy S, Jodeh H.A, Lakhrissi K, Toumiat H.O, (2016). Corrosion inhibition of mild steel in hydrochloric acid by 5,5',5''-(nitriлотris (methylene)) tris-(8-quinolinol):Experimental, theoretical and molecular dynamic studies. Moroccan Journal of Chemistry, Vol. 4, No. 2, pp.592-612
- Loto CA (2011). Inhibition effect of tea (*Camellia Sinensis*) extract on the corrosion of mild steel in dilute sulphuric acid. Journal of Materials and Environmental Science, 2, 33-344.
- Laxmi K., (2014). Theoretical Approach on structural aspects of antiepileptic agent indoline-2,3-dione-3-oxime by arguslab 4 software, J. Appl. Chem., Vol. 2, No.1, pp. 92-101,
- Lahodny-Sarc O, Kapor F, (2002). Corrosion inhibition of carbon steel in the near neutral media by blends of tannin and calcium gluconate, Mater. Corros., Nol. 53, No. 4, 264–268. 11
- Leon-Silva U, Nicho M, Gonz'alez-Rodr'iguez J, Chac'on-Nava J and Salinas-Bravo VJ 2010. Solid State Electrochem.,14, 1089–1100.
- Martinez, S, and Tagljar I, (2003). Correlation between the molecular structure and the corrosion inhibition efficiency of chestnut tannin in acidic solutions, Journal of Molecular Structure: THEOCHEM. 640: 167-174.
- Michael S., Bob F., Audrey T., Jepsun W.P. (2000), Corrosion inhibition of wet gas pipelines under high gas liquid velocity, NACE international 2000
- Musa AY, Kadhum AH, Mohamad AB, Rahoma AB and Mesmari H, 2010. Electrochemical and quantum chemical calculations on 4, 4-dimethyloxazolidine- 2-thione as inhibitor for mild steel corrosion in hydrochloric acid, J. Mol. Struct., Vol. 969, No. 1, pp. 233-237
- Nwosu J.N., (2012). The Rheological and Proximate Properties of some food thickeners ("Ukpo" "Achi" and "Ofo") as affected by processing, Int. J. of Basic and Applied Sci. Vol.1 No. 4, pp.304
- Ndukwe M.C., (2009), Determination of Selected Physical Properties of *Brachystegia eurycoma* seeds, Research Agric. Engr. 55, pp 165-166
- Onukwube N.D, Awomukwu D.A, and Brown N. (2016). Inhibition of corrosion of mild steel in alkaline medium by ethanol extract of *Pterocarpus Soyauxii* Taub leaves. Ewemen Journal of Analytical & Environmental Chemistry: Vol. 2(1) Pg. 38 - 44
- Okafor P.C, Ikpi M.E, Ebenso E.E, Ekpe U.J, and Umoren S.A, (2008). Inhibitory action of *Phyllanthus amarus* extracts on the corrosion of mild steel in acidic medium, Corros. Sci. 50, pp. 2314-2315
- Obi-Egbedi N.O, Obot I.B, El-Khaiary M.I, Umoren S.A and Ebenso E.E, (2011). "Computational Simulation and Statistical Analysis on the Relationship between Corrosion Inhibition Efficiency and Molecular Structure of Some Phenanthroline Derivatives on Mild Steel Surface," Int. J. Electrochem. Sci., vol. 6, pp. 5649-5675
- Obot I.B, Macdonald D.D, and Gasem, Z.M, (2015). Corrosion Science. 99:1.
- Okoronkwo A.E, Olusegun S.J and Olaniran O. (2015). Acid extract of *Gliricidia sepium* leaves as green corrosion inhibitor for mild steel in HCl solutions, African corrosion Journal. Vol.1, 30-35.
- Oguzie E.E, Onuchukwu, A.I, Okafor P.C, and Ebenso E. E. (2006). Corrosion inhibition and adsorption behaviour of *Ocimum basilicum* extract on

aluminium. *Pigment and Resin Technology*, 35, 63–70. <http://dx.doi.org/10.1108/03699420610652340>

Peter A and Sharma SK 2017. Use of *Azadirachta indica* (AZI) as green corrosion inhibitor against mild steel in acidic medium. *International Journal of Corrosion Scale Inhibition.*, 6(2), 112-131.

Parr, RG, Szentpaly L, Liu S, (1999). Electrophilicity Index, *Journal of American Chemical Society*, 121: 1922-1924. Pearson RG, *coordination Chemistry Review*, 1990. 100:403

Peter A, Sanjay K.S and Ime B.O (2016). Anticorrosive efficacy and adsorptive study of guar gum with mild steel in acidic medium, *Journal of Analytical Science and Technology*, 7:26 DOI 10.1186/s40543-016-0108-3

Rozenfeld I. L. (1981). *Corrosion Inhibitors*. McGraw–Hill, New York.

Thompson M.A. (2004). Molecular docking using ArgusLab, an efficient shape-based search algorithm and Ascore scoring function, in *Proc. ACS Meeting*, Philadelphia, Pa, USA, p. 172,

Uzoma A., Odusanya O.S. (2011). *Mucuna sloanei*, *Datarum microcarpum*, and *Brachystegia eurycoma* starch-hydrocolloids system, *Afri. J. of Food Sci.* vol. 5(13), pp. 733-740

Umoren S.A, Obot I.B, Ebenso E.E, Okafor P.C, Ogbobe O, Oguzie E.E (2006a). Gum Arabic as a potential corrosion inhibitor for aluminium in alkaline medium and its adsorption characteristics. *Anti-corrosion Methods & Material*, 53:277-282.

Umoren S.A, Ogbobe O, Ebenso EE, Ekpe U.J (2006b). Effect of halide ions on the corrosion inhibition of mild steel in acidic medium using polyvinyl alcohol. *Pigment and Resin Technol.* 35: 284 –292.

Umoren S.A, Ebenso E.E, Okafor P.C, Ekpe U.J, Ogbobe O. (2007). Effect of halide ions on the corrosion inhibition of aluminium in alkaline medium using polyvinyl alcohol. *J.Appl.Polymer Sci.* 103: 2810-2816

Umoren SA, Obot IB., Ebenso EE., Okafor PC (2008). Eco-friendly inhibitors from naturally occurring exudate gums for Aluminium corrosion inhibition in acidic medium, *Port. Electrochim. Acta* v.26 n.3

Ulaeto S.B, Ekpe U.J, Chidiebere M.A, Oguzie E.E (2012), Corrosion Inhibition of mild steel in hydrochloric acid by acid extracts of *Eichhornia crassipes*, *Int. J. of material Chem.* 2(4), pp.158-164

Verma S.A. and Mehta M.N. (1997). “Effects of acid extracts of powered seeds of *Eugenia Jambolans* on corrosion of mild steel in HCl-study by DC polarisation techniques,” *Transactions of the Society for Advancement of Electrochemical Science and Technology*, 32 (4), 89–93.

Verma S.A. and Mehta M.N. (1997). “Effects of acid extracts of powered seeds of *Eugenia Jambolans* on corrosion of mild steel in HCl-study by DC polarisation techniques,” *Transactions of the Society for Advancement of Electrochemical Science and Technology*, 32 (4), 89–93.

Wang Z. (2012). The inhibition effect of bis-benzimidazole compound for mild steel in 0.5 M HCl solution. *Int. J. Electrochem. Sci.* 7, 11149-11160

Samuel N, Ogah S.P.I, Obike A, Igwe J.C, Ogbonna I.V (2015). Investigation of the Inhibitory Action of *Brachystegia eurycoma* (Achi) Seed Extracts on the Corrosion of Mild Steel in 2M HCl by Method of Weight Loss. *International Journal of Scientific Research and Education*. Vol. 3, P 3744-3753,

Shubham K, Sanjiv K, Kalavathy R, Siong M.L, Syed A.A.S, Hari O and Balasubramanian N. (2018). Synthesis, biological evaluation and corrosion inhibition studies of transition metal complexes of Schiff base. *Chemistry Central Journal.*, 12:117

Stewart J.J.P. (2013). Optimization of parameters for semiempirical methods VI: more modifications to the NDDO approximations and re-optimization of parameters, *J. Mol. Model.*, Vol. 19, no. 1, pp. 1–32.

Soltani N, Tavakkoli N, Khayatkashani M, Jalali M.R, Mosavizade A, (2012). Green Approach to Corrosion Inhibition of 304 Stainless Steel in Hydrochloric Acid Solution by the Extract of *Salvia officinalis* leaves, *Corros. Sci.*, Vol. 62, pp. 122- 135,

Schmit G, (2000). Drag Reduction- a widely neglected property of corrosion inhibitors, proceedings of the 9<sup>th</sup> European symposium of corrosion and scale inhibitor.

Stewart J.J.P, (1989). Optimization of parameters for semiempirical methods I. Method, *J. Comput. Chem.*, vol.10, no. 2, pp. 209

Singh A, Ansari K.R, Kumar A, Liu W, Song C, Lin Y. (2017). Electrochemical, surface and quantum chemical studies of novel imidazole derivatives as corrosion inhibitors for J55 steel in sweet corrosive environment. *Journal of Alloys and Compounds.* 712:121-133

Shockry H, Yuasa M, Sekine I, Issa R.M, El-baradie H.Y, Gomma G.K (1998). Corrosion inhibition of mild steel by Schiff base compounds in various aqueous solutions. Part I. *Corros. Sci.*, 40:2173 – 2186.

Yiguang W, Welfeng F, Linan A, (2006). Oxidation/Corrosion of Polymer-Derived SiAlCN Ceramics in water, *Journal of the American Chemical Society*, Vol. 89, Issue 3, pg. 1079-1081

Zhang Z, Tian N, Zhang W, Huang X, Ruan L, Wu L. (2016). Inhibition of carbon steel corrosion in phase-change materials solution by methionine and proline. *Corrosion Science.* 111:675-689